INTERNATIONAL JOURNAL OF
ENERGY RESEARCH WILEY

Channel formation and visualization of melting and crystallization behaviors in direct-contact latent heat storage systems

Sven Kunkel[1] | **Philipp Schütz[2]** | **Frederik Wunder[1]** 🟢 | **Stefan Krimmel[2]** 🟢 | **Jörg Worlitschek[2]** | **Jens-Uwe Repke[3]** | **Matthias Rädle[1]**

[1]Center for Mass Spectrometry and Optical Spectroscopy, Hochschule Mannheim—University of Applied Sciences, Mannheim, Germany

[2]Competence Centre for Thermal Energy Storage, Hochschule Luzern—University of Applied Sciences and Arts, Horw, Switzerland

[3]Dynamics and Operation of Technical Systems, Technische Universität Berlin, Berlin, Germany

Correspondence
Frederik Wunder, Center for Mass Spectrometry and Optical Spectroscopy, Hochschule Mannheim—University of Applied Sciences, Paul-Wittsack-Straße 10, Mannheim 68163, Germany.
Email: f.wunder@hs-mannheim.de

Summary
Thermal storage systems are an essential component for increasing the share of renewable energies in residential heating and for the valorization of waste heat. A key challenge for the widespread application of thermal storage systems is their limited power-to-capacity ratio. One potential solution for this challenge is represented by direct-contact latent heat storage systems, in which a phase change material (PCM) is in direct contact with an immiscible heat transfer fluid (HTF). To demonstrate the applicability of the direct-contact concept for domestic hot water production, a PCM with a phase change temperature of 59°C is chosen. To enable cost-efficient implementation of the storage system, a eutectic mixture of two salt hydrates, magnesium chloride hexahydrate and magnesium nitrate hexahydrate, is chosen as the PCM. One key aspect for the direct-contact concept is that, during discharge, the HTF channels in the PCM do not become clogged during the solidification of the PCM. In this study, the formation and topology of the channels in direct-contact systems under an optimized flow condition are investigated via visual observation and X-ray computed tomography. The elucidation of the channel structure provides information on the melting and crystallization behaviors of the PCM, which are shown schematically.

KEYWORDS
computed tomography, direct contact latent heat storage, heat transfer surface, latent heat storage, phase change material, thermal heat storage

1 | INTRODUCTION

Because of the increasing demand for energy, the finite nature of fossil fuels, and concerns about environmental impacts, it is necessary to increase the use of renewable energy sources such as solar, biomass, and wind energies. Because of their temporary nature, the effective use of these energy sources depends on the availability of efficient energy storage systems.[1] Because of the natural variability of sun and wind as heat and electricity sources, an effective storage technology is required to compensate for the time lag between energy supply and demand.[2]

In this investigation, we focus on thermal storage systems. There are three types of thermal energy storage systems: sensible heat storage, latent heat storage, and thermochemical heat storage systems.[3] Despite their high energy storage densities of the reactants of approximately 500 kWh/m^{3}, thermochemical storage systems have a major disadvantage in that the technology is complex and requires large investments.[4,5] In comparison with sensible heat storage systems, latent heat storage systems have the following advantages[6]:

- Extraction and supply of thermal energy at an approximately constant temperature
- Approximately five times higher energy storage density ($\Delta\vartheta = 10$ K)

For a solid/liquid phase change, phase change materials (PCMs) can be subdivided into two main categories: inorganic and organic substances.[7] Inorganic substances include salt hydrates, salts, metals, and alloys, while organic substances include paraffins, nonparaffins, and polyalcohols. Organic nonparaffins include a variety of substances such as fatty acids. In addition, eutectic mixtures of inorganic and/or organic substances are also used as PCMs.[8] A large number of organic and inorganic substances have melting points in a technically relevant range and substantial enthalpies of fusion. Nevertheless, besides having a suitable melting point, the majority of PCMs does not meet the criteria for a suitable storage medium[9] as their enthalpy of fusion is too low or they are corrosive or simply too expensive. A recent overview of suitable PCMs is given in Zalba et al.[10] In this study, we focus on salt hydrates. Similarly, to paraffins and fatty acids, they have melting temperatures between 0°C and 100°C. Fatty acids were excluded because they are about three times more expensive than paraffins.[8] Compared with paraffins, salt hydrates have several advantages[11]:

- High volumetric latent heat storage capacity (approximately 200-600 kJ/L[3])
- Low cost and widespread availability
- Sharp phase change (paraffins are mixtures of several hydrocarbons and thus have a melting temperature range rather than a sharp melting point as in the case of salt hydrates[8])
- High thermal conductivity (paraffin of approximately 0.2 W/m²·K[12] and salt hydrates of approximately 0.5 W/m²·K[13])
- Nonflammable

However, salt hydrates also have some disadvantages, which make their use as a latent heat storage mediums more difficult[10]:

- Undercooling: The liquid PCM cools to below the melting point of the PCM during energy removal without solidifying.
- Phase separation can occur in PCMs that consist, for example, of several components. During a melting and crystallization cycle, it is possible that phases partially separate. The individual phases have different properties, which also differ from the desired properties of the PCM.
- Corrosion: Many inorganic substances, as well as salt hydrates, are corrosive towards metals. This must be considered during the construction of the storage tank.
- Water sorption due to the hygroscopy behavior in many salt hydrates leads to changes of the stoichiometric water content reducing the phase change enthalpy.

To improve the performance of latent heat storage systems with salt hydrates as PCMs, nucleating agents and thickeners help to prevent both undercooling and phase separation.[1] In 1957, Etherington suggested another solution for the problems of undercooling and phase separation.[14] In this approach, the storage material, the salt hydrate (disodium phosphate dodecahydrate), and the heat transfer fluid (HTF) (oil) are in direct contact, and the media are not miscible. The HTF is injected into the lower part of the storage tank and rises through the liquid PCM in the form of droplets, as the density of the HTF is lower than that of the PCM. Because of the resulting agitation, undercooling and phase separation of the PCM are reduced.
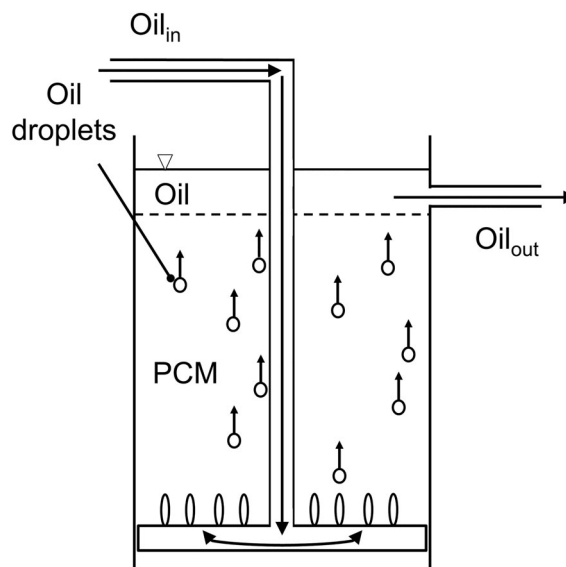

FIGURE 1 Schematic illustration of a direct-contact latent heat storage system[15]

In this study, a direct-contact latent heat storage system employing a eutectic mixture of two salt hydrates as the PCM, namely, magnesium chloride hexahydrate and magnesium nitrate hexahydrate, and a mineral oil as the HTF is investigated. Figure 1 illustrates a direct-contact latent heat storage tank.

In Figure 1, the PCM is in a completely melted state; that is, the storage system is loaded. If oil at a temperature below the melting temperature of the PCM is injected into the storage tank, the PCM cools down and begins to crystallize in the vicinity of the oil droplets. During this crystallization process, a channel structure is formed in the PCM. If the PCM is completely crystallized, a channel structure remains within the PCM. In this state, the storage tank is discharged. To charge the system again, oil at a temperature above the melting temperature of the PCM is pumped through the channel structure to liquify the PCM.

Besides direct-contact systems, indirect-contact latent heat storage systems have also been described in the literature.[16-18] In these systems, the PCM and the HTF are physically separated by a wall. For instance, a piping system for the HTF separates it from the PCM. Compared with indirect heat transfer, direct heat transfer offers the following advantages[3,19,20]:

- Higher charging and discharging rates due to improved heat transfer between the PCM and the HTF
- Higher storage density, since there is no piping system in the storage tank
- Extended period of high transfer rate during charge because solidified PCM with low thermal conductivity around the piping system does not screen the heat transfer

Further studies on direct-contact latent heat storage systems are described in the literature.[14,15,20-37] In these studies, only a few simplified descriptions of the melting and crystallization behaviors are given.[34,36] In particular, the determination of heat transfer surfaces has not been described.

To support a deeper understanding of direct heat transfer and the design of the storage system, this study provides a detailed explanation of the melting and crystallization behaviors of the PCM. The investigation is based on volumetric images from the HTF channels recorded by X-ray computed tomography (CT). The heat transfer surface is then subsequently determined directly from the images for one model storage tank. For the design of the storage tanks, however, it is of interest to understand how the heat transfer surface is distributed in the PCM. This allows conclusions to be drawn about which areas melt quickly and which areas melt slowly. To facilitate the X-ray analysis, a model storage tank was built, which has only one oil inlet at the bottom. The internal surface area is an important property for any heat exchanger, therefore this studies goal is to advance the design and scale up of direct-contact PCM heat storage systems.

2 | MATERIAL AND METHODS

2.1 | Phase change material

The PCM used was a stable eutectic mixture of the two salt hydrates: magnesium chloride hexahydrate and magnesium nitrate hexahydrate. The PCM has a melting point of 59°C and is well suited for storing heat from renewable energy sources or for storing low-temperature waste heat. The mineral oil Fragoltherm Q-7, which is optimized for cooling and heating in process engineering plants, was employed as an HTF. Table 1 shows the properties of the PCM and the mineral oil.

The support material of the storage tank is also required for the investigation of the channel structure by means of X-ray CT. Therefore, polycarbonate was selected for this purpose.

2.2 | Experimental setup and measurement method

The experimental setup shown in Figure 2 was used for the investigation of the channel geometry. The setup consists of an oil receiver tank (A), an electrical gear pump

TABLE 1 Material properties of the PCM and mineral oil as the heat transfer fluid (HTF)

|	PCM	Oil
Melting point, °C	59[38]	Less than −40
Heat of fusion, kJ/kg	132.2[38]	Not relevant
Heat capacity solid, kJ/kg·K	1.86 (40°C)[38]	Not relevant
Heat capacity liquid, kJ/kg·K	2.42 (70°C)[38]	2.257 (70°C)[40]
Heat conductivity solid, W/m·K	0.678 (53°C)[38]	Not relevant
Heat conductivity liquid, W/m·K	0.510 (65°C)[38]	0.123 (70°C)[40]
Density liquid, kg/m³	1550[38]	797 (70°C)[40]
Density solid, kg/m³	1630[38]	Not relevant
Viscosity, mPa·s	35 (62.5°C)[39]	4.51 (50°C)[40]

Abbreviation: PCM, phase change material.
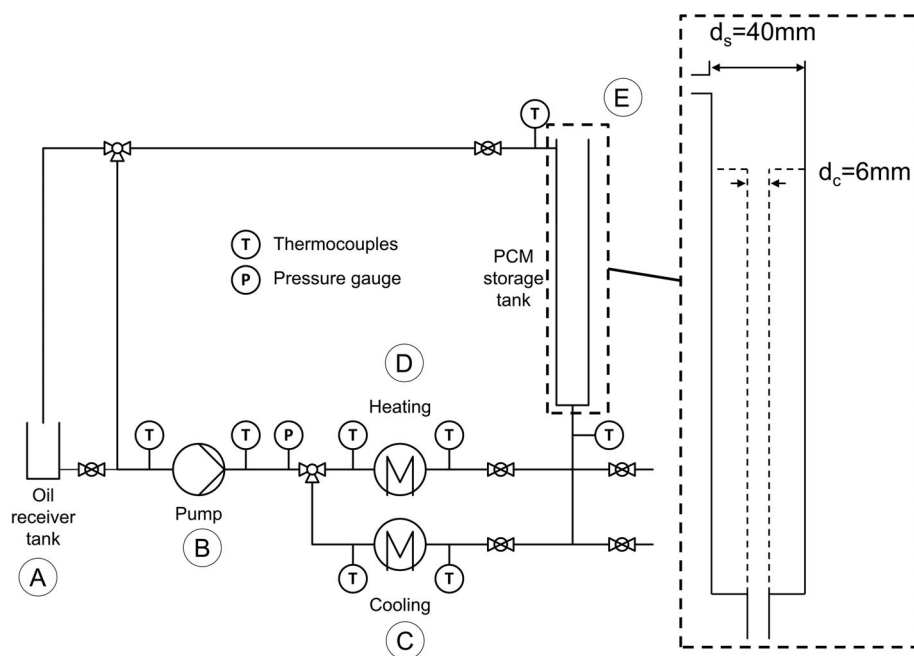
FIGURE 2 Schematic of the experimental setup[37]: A, oil receiver tank; B, pump; C, cooling; D, heating; E, storage tank

(B) delivering a pressure drop-independent mass flow, two heat exchangers (C and D), and the storage tank (E) containing the PCM. The storage tank is made of transparent polycarbonate and has a height of 350 mm and an internal diameter of 40 mm. The transparent polycarbonate makes it possible to observe the melting and crystallization behaviors. At the bottom of the storage tank, there is one orifice with a diameter of 6 mm, which allowed the input of oil into the storage tank. Two different channel configurations were investigated: an artificially created cylindrical channel and a channel under real flow conditions. The artificial cylindrical channel had a diameter of 6 mm and was created using a cylindrical inset. This channel geometry serves as a validation method for the measurement and evaluation method, as the shell surface can be calculated based on the known geometry.

To measure the pressure and oil temperature in the pipeline, a pressure transmitter and eight thermocouples (type K) were integrated. To create the artificial cylindrical channel, a steel pipe with an outer diameter of 6 mm was inserted into the oil inlet opening in the bottom of the storage tank containing the liquid PCM. Subsequently, oil was introduced at a temperature below the melting point of the PCM, such that the PCM began to crystallize on the wall of the steel pipe. Once the entirety of the PCM had crystallized, it was possible to remove the pipe, and a channel with an inner diameter of 6 mm remained inside the PCM. To create a channel under real flow conditions, complete melting of the PCM is required. The PCM was overheated to a temperature of approximately 68°C, and oil at a temperature of 49°C was then injected into the storage tank. The oil mass flow was set to $6.50 \cdot 10^{-4}$ kg/s. The PCM then cooled down to its melting point, and crystallization began. In this case, a branched channel structure is formed within the PCM. To investigate the channel structure, the entire storage tank was removed from the experimental setup. Subsequently, the channel structure was investigated by means of X-ray CT. The XT H 225 ST CT system from Nikon was used for this purpose. The X-ray radiation was generated with a rotating anode tube with a maximum acceleration voltage of 225 kV. For the measurement of the storage system, an acceleration voltage of 120 kV and a tube current of 550 μA were employed. The storage system was measured in two overlapping segments (top and bottom), with a field of view of 2000 × 2000 pixels recorded by the X-ray detector. The cross-sectional images were subsequently reconstructed by the Nikon reconstruction software, based on the Feldkamp-Davis-Kress algorithm.[41]

The dimension of the storage tank resulted in a resolution of 93 μm. After the measurement started, the sample stage rotated 360°, and images were taken continuously during the measurements. After approximately 38 minutes, the measurement was finished.

The images of the two consecutive measurements were then combined manually by matching the two image stacks according to position and prominent features.

2.3 | Evaluation method

The volumetric images were analyzed by the Volume Graphics Studio Max 3.1.2 software from Volume

Graphics (Heidelberg, Germany). The channel visualization and analysis of the heat transfer surface were performed with the inclusion module. The selection threshold for the analysis process was based on the integrated automatic threshold procedure. The program myVGL from Volume Graphics was subsequently employed to measure and display individual channel-specific conditions, such as the local diameter of the channel.

3 | RESULTS AND DISCUSSION

3.1 | Channel formation during solidification

Figure 3 shows the crystallization behavior schematically.

At the beginning of the solidification behavior, the PCM is completely melted, and the oil rises in the PCM in the form of droplets (Figure 3A). The oil enters the storage tank in the form of a jet, which is followed by decay of the jet. After the decay, single oil droplets are formed. By introducing oil at a temperature below the phase change temperature of the PCM, the PCM begins to cool down. Subsequently, the PCM starts to solidify, whereby some solid PCM particles form in the liquid PCM. In addition, a layer of solid PCM is formed at the PCM/oil phase boundary at the upper part of the storage tank. This layer appears as a kind of foam. The remaining portion of the solid PCM is kept in suspension by the oil flow. Some solid PCM particles sink to the bottom of the storage tank because the solid particles have a higher density than that of the liquid PCM. In the lower part of the storage tank, the oil jet forms a single cylindrical channel. Over time, an increasing amount of solid PCM particles are formed, which are kept in suspension (Figure 3B). Because of the formation of solid PCM particles, the oil flow is hindered; this flow resistance increases with height in the storage tank. Nevertheless, in the middle of the storage tank, the jet decay can still form a strongly branched channel structure. However, in the top part, the hindrance is so strong that only a main channel is formed. Finally, the PCM solidifies completely (Figure 3C).

In order to determine the channel structure, the solidified storage tank was transferred to an X-ray CT system where a stack of volumetric images were obtained and recombined. Figure 4 shows the channel structures of the artificial cylindrical channel (Figure 4A) and of one channel under real flow conditions (Figure 4B) within the PCM, obtained by means of the CT system.

Figure 4 shows a visualization of the channels extracted from the X-ray CT images. Figure 4A displays the storage system with the artificial cylindrical channel. The optical analysis revealed that the average diameter was 6.20 mm ($\pm$0.08 mm) and the shell surface was 93.65 cm^2. With a height of 319 mm, the surface area of the shell should therefore be 62.13 cm^2 ($\pm$6.55 cm^2). The discrepancy with the measured shell surface can be explained by the surface roughness of the channel wall. Figure 4B presents the visualization of the structure of the channel, which was created under real flow conditions. Beginning at the oil inlet, a nearly cylindrical section of the channel with a height of approximately 90 mm and a diameter of approximately 2.4 mm ($\pm$0.2 mm) can be observed. The heat transfer surface was approximately 6.8 cm^2. This section is generated by the oil jet resulting from the oil mass flow. The jet then decays, which causes a branch to form within the PCM. In the next section (beginning at a height of about 110 mm), the structure is heavily branched. It is in this section that the largest heat transfer area is provided. This section is succeeded by another (between 260 and 320 mm), in which the individual branched channels reconnect. The number of branches is thereby reduced. In contrast to previously reported findings,[36] an uneven channel structure was formed. This structure fundamentally influences the melting of the PCM. In this example, the shell surface of the channel was 168.1 cm^2, which also corresponds to the heat transfer surface.

FIGURE 3 Schematic illustration of the crystallization behavior of the phase change material (PCM) in three different phases: A, initial situation, where PCM is completely melted; B, intermediate situation, where solid and liquid phases of the PCM coexist; C, storage tank in the discharged state, where PCM is solid
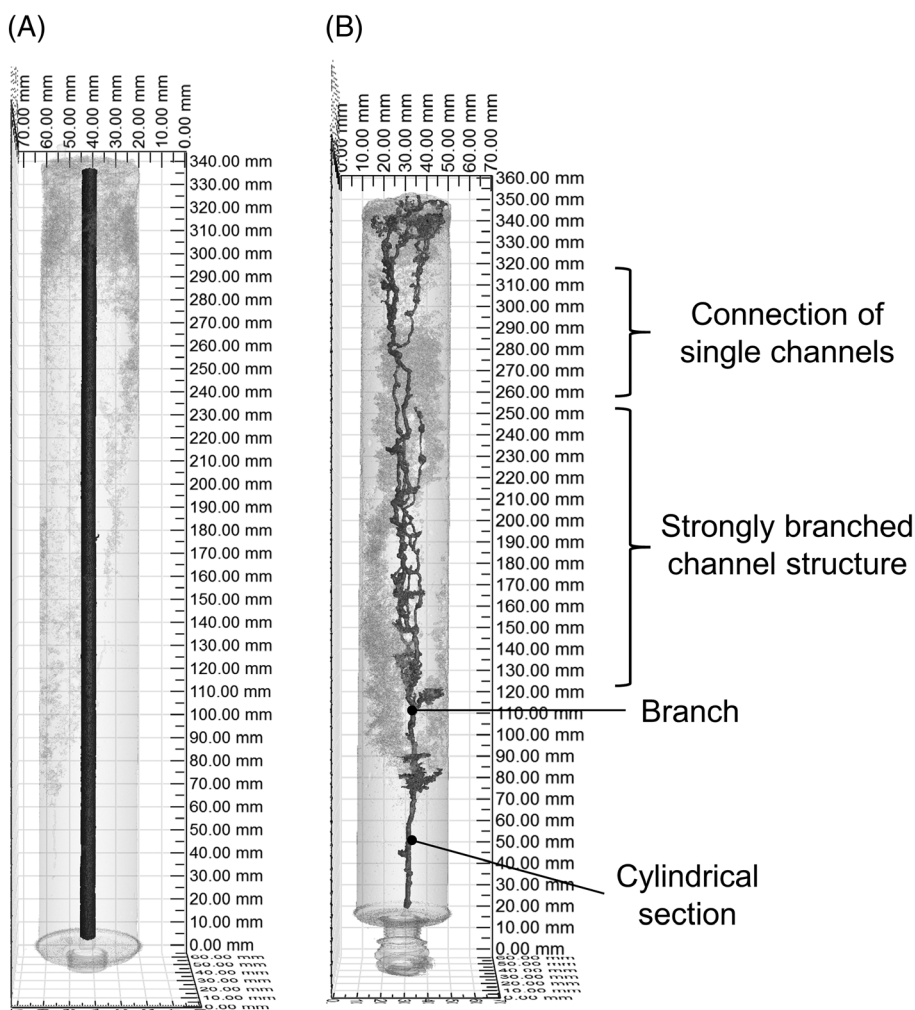
(A) (B)
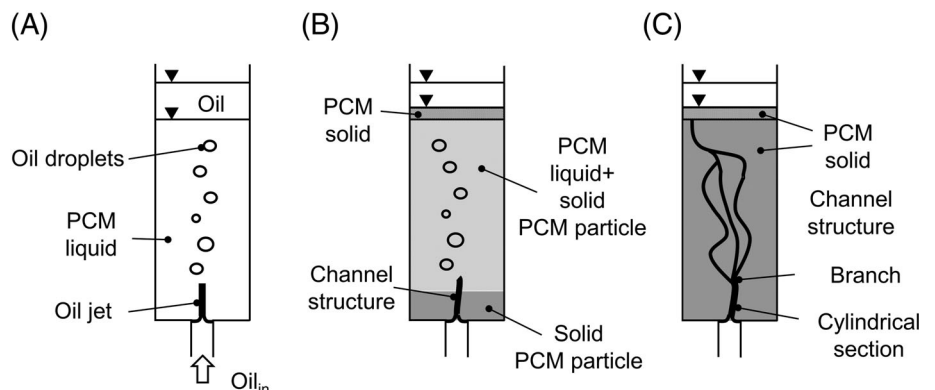
FIGURE 4 Visualization of the structures formed under real flow conditions within the phase change material (PCM), obtained by means of the X-ray computed tomography (CT) system of the following: A, the artificial cylindrical channel; B, a channel

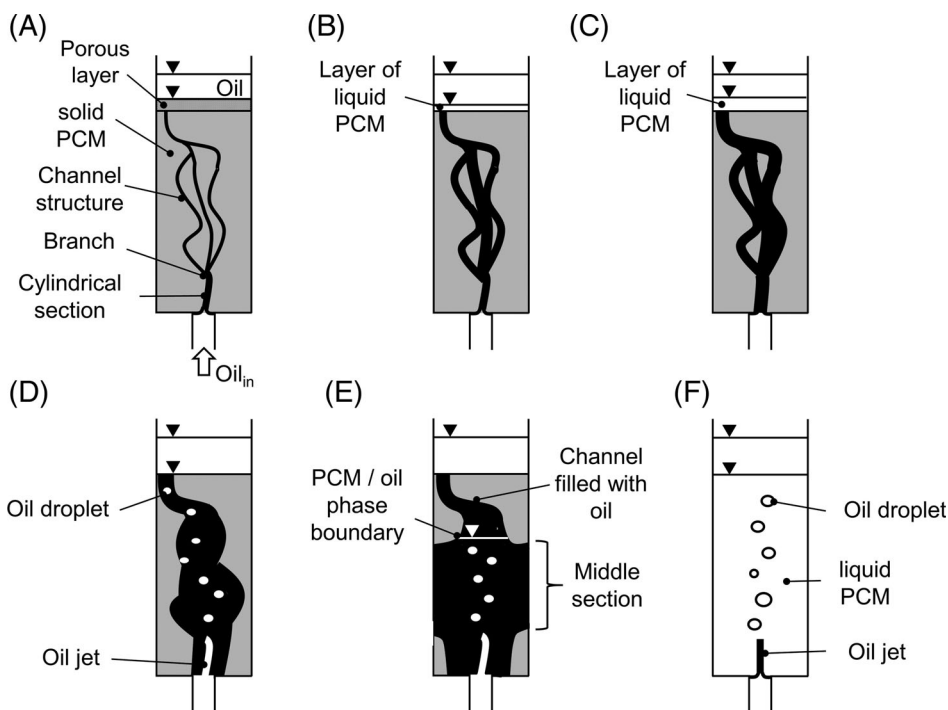(A) (B) (C)

(D) (E) (F)

FIGURE 5 Schematic illustration of the melting behavior of the phase change material (PCM) divided into six different phases. A, Initially, the PCM is completely solid. B, The channel structure expands via melting of the PCM and formation of a liquid PCM layer at the channel outlet. C, The channel structure expands further, and the liquid PCM layer at the channel outlet grows as well. D, The threshold diameter is reached, at which point the liquid PCM flows back into the channel structure. E, In the melting process, the middle section melts first. F, The storage tank is then in a charged state, wherein the PCM is liquid
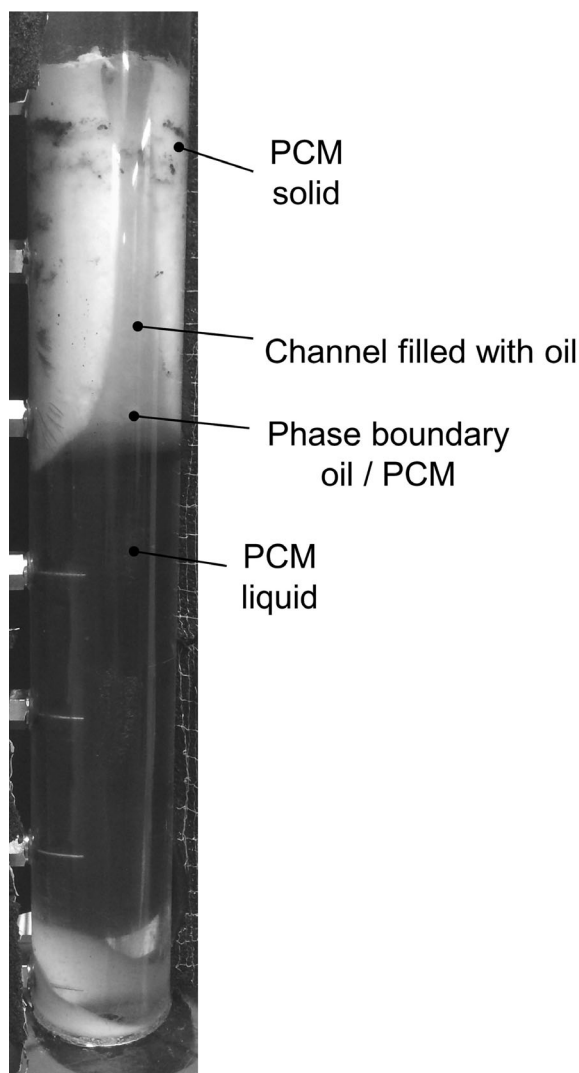
FIGURE 6 Image of the state illustrated in Figure 5E

3.2 | Melting behavior

Figure 5 schematically shows the melting behavior of the PCM.

At the beginning of the charging process, the PCM is completely solidified, and a channel structure is present within the PCM. The oil then flows through the prevalent channel structure, and the channels are completely filled with oil (Figure 5A/Figure 3C). By injecting oil with a temperature above the melting temperature of the PCM into the system, the PCM heats up and begins to melt. Convective heat transfer occurs, and the channel structure expands. The oil flow partially removes liquid PCM from the canal. This results in the formation of a liquid PCM layer at the channel outlet (Figure 5B). The channel structure continues to expand, and the layer of liquid PCM also continues to grow (Figure 5C). If the channel structure reaches a threshold diameter, the layer of liquid PCM flows back into the channel structure. The channels are then

filled with liquid PCM. In consequence, an oil jet forms, which is followed by decay of the jet and the formation of single oil droplets. The liquid PCM is further heated by the oil, while the liquid PCM melts the solid PCM via conductive heat transfer (Figure 5D). Further areas of the PCM are melted by this additional supply of heat. From optical recordings of the charging process, it can be seen that the middle section of the storage system first melts completely, followed by the lower section. The PCM/oil phase boundary is within the channel structure (Figure 5E). Eventually, the top section is melted until the entire PCM is in the liquid state (Figure 5F). Figure 6 shows a photograph of the intermediate state illustrated in Figure 5E.

Figure 6 confirms that the PCM in the middle section of the storage tank had already melted while the PCM in the top and bottom sections was still solid. From a qualitative point of view, this state provides the largest heat transfer surface. Although the heat transfer surface is reduced in comparison with the middle section, the lower part of the PCM melts subsequently. This may be explained by the high heat flux in this area due to the highest temperature gradient between the oil and PCM. Finally, the PCM in the top section melts as the rest of the PCM is already liquid. The individual channels have merged by this stage, to form a main channel. The heat transfer surface is small.

Previous studies have described and discussed,[20,31] among other things, the melting and crystallization behaviors of PCMs. This publication supports our finding that the middle section melts first. These results suggest that an efficient storage system should have a low height in order to reduce the area in the top section of the storage tank wherein PCM is solid (Figure 6). As a conclusion, it can be said that direct-contact latent heat storage tanks should be built wider rather than taller. It is not expected that the residence time of the oil within the PCM would be insufficient to achieve efficient heat transfer in shorter systems. A direct-contact latent heat storage system employing erythritol (density[42]: 1480 kg/m^3) and an oil as the HTF has been described previously.[36] In this study, it was shown that efficient heat transfer can be achieved even with PCM heights as low as 0.2 m.

For initial designs, a total PCM height of approximately 0.30 m is therefore recommended, even for larger storage tanks.

4 | CONCLUSIONS

In this study, the melting and solidification behaviors of a PCM within a direct-contact latent heat storage system were experimentally investigated. The considered system consisted of a vertical cylindrical storage tank containing a eutectic mixture of two salt hydrates as the PCM and

a mineral oil as the HTF. By combining visual observations with a volumetric cross-sectional analysis by X-ray CT, the melting and solidification behaviors were elucidated, and design principles for such storage systems were visualized, derived, and proposed. The conclusions are summarized as follows.

Visual and X-ray CT inspections confirmed a hierarchical melting behavior. The middle section of the PCM melted first, followed by the bottom section, and finally the top section. During the solidification behavior, a channel structure providing an increased heat transfer surface is formed in the middle section. The total surface area was 168.1 cm^2 in the investigated geometry.

The X-ray CT images confirmed that the channel structure was divided into three sections: an unbranched section in the lower part of the PCM, succeeded by a strongly branched section in the middle, and a less branched section at the upper part. With the help of these images, the melting and crystallization behaviors were illustrated in detail.

For the design of direct-contact latent heat storage systems, it is recommended to build storage systems wider rather than taller, as the channel structure in the upper part of the PCM is less branched and the heat transfer surface is thereby reduced. This can lead to delayed melting and reduced storage performance.

The elucidation of the melting and crystallization dynamics was an important undertaking to deepen the understanding of direct heat transfer and will assist greatly in the design of direct-contact latent heat storage systems.

ACKNOWLEDGEMENTS

NOMENCLATURE

d_c diameter of the PCM channel (mm)
d_s diameter of the storage tank (mm)

ABBREVIATIONS

CT   computed tomography
HTF   heat transfer fluid
P   pressure gauge
PCM   phase change material
T   thermocouple

ORCID

Frederik Wunder https://orcid.org/0000-0003-3990-8297

Stefan Krimmel https://orcid.org/0000-0002-5462-2548

REFERENCES

1. Dincer I, Rosen MA. *Thermal Energy Storage: Systems and Application*. Second ed. United Kingdom: Wiley; 2011.
2. Tamme R, Jossen A, Henning H-M. Speichertechnologien für erneuerbare energien—voraussetzung für eine nachhaltige energieversorgung, FVS Themen; 2006; http://www.fvee.de/fileadmin/publikationen/Themenhefte/th2006/th2006_03_03.pdf. (Stand: October 31, 2018).
3. Mehling H, Cabeza LF. *Heat and Cold Storage With PCM*. Berlin: Springer-Verlag; 2008.
4. Pardo P, Deydier A, Anxionnaz-Minvielle Z, Rouge S, Cabassud M, Cognet P. A review on high temperature thermochemical heat energy storage. *Renew Sustain Energy Rev*. 2014;32:591-610.
5. Pintaldi S, Perfumo C, Sethuvenkatraman S, White S, Rosengarten G. A review of thermal energy storage technologies and control approaches for solar cooling. *Renew Sustain Energy Rev*. 2015;41:975-995.
6. Nomura T, Okinaka N, Akiyama T. Technology of latent heat storage for high temperature application: a review. *ISIJ Int*. 2009;50(9):1229-1239.
7. Abhat A. Low temperature latent heat thermal energy storage: heat storage materials. *Sol Energy*. 1983;30:313-332.
8. Hasnain SM. Review on sustainable thermal energy storage technologies, part I: heat storage materials and techniques. *Energ Conver Manage*. 1998;39:1127-1138.
9. Sharma A, Tyagi VV, Chen CR, Buddhi D. Review on thermal energy storage with phase change materials and applications. *Renew Sustain Energy Rev*. 2009;13:318-345.
10. Zalba B, Marín JM, Cabeza LF, Mehling H. Review on thermal energy storage with phase change: materials, heat transfer analysis and applications. *Appl Therm Eng*. 2003;23:251-283.
11. Kuznik F, David D, Johannes K, Roux J-J. A review on phase change materials integrated in building walls. *Renew Sustain Energy Rev*. 2011;15:379-391.
12. Farid MM, Khudhair AM, Razack SAK, Al-Hallaj S. A review on phase change energy storage: materials and applications. *Energ Conver Manage*. 2004;45:1597-1615.
13. Lele AF, N'Tsoukpoe KE, Osterland T, Kuznik F, Ruck WKL. Thermal conductivity measurement of thermochemical storage materials. *Appl Therm Eng*. 2015;89:916-926.
14. Etherington TL. A dynamic heat storage system, heating piping and air conditioning; 1957.
15. Kunkel S, Kübel-Heising F, Dornhöfer P, et al. Direktkontakt-latentwärmespeicher zur effizienzsteigerung von wärmepumpen. *Chem Ing Tech*. 2018;90:234-240.
16. Zhang S, Zhang L, Yang X, et al. Experimental investigation of a spiral tube embedded latent thermal energy storage tank using paraffin as PCM. *Energy Procedia*. 2017;105:4543-4548.
17. Tay NHS, Belusko M, Bruno F. Experimental investigation of tubes in a phase change thermal energy storage system. *Appl Energy*. 2012;90:288-297.
18. Cabeza LF, Ibáñez M, Solé C, Roca J, Nogués M. Experimentation with a water tank including a PCM module. *Sol Energy Mater Sol Cells*. 2006;90:1273-1282.
19. Nagano K, Takeda S, Mochida T, Shimakura K. Thermal characteristics of a direct heat exchange system between granules with phase change material and air. *Appl Therm Eng*. 2004;24:2131-2144.

20. Wang W, Guo S, Li H, et al. Experimental study on the direct/indirect contact energy storage container in mobilized thermal energy system (M-TES). *Appl Energy*. 2014;119: 181-189.

21. Edie DD, Melsheimer SS, Mullins JC. Immiscible fluid—heat of fusion heat storage system. Paper presented at: Sharing the Sun: Solar Technology in the Seventies, Proceedings of the Joint Conference; Winnipeg; 1976; 391-399.

22. Edie DD, Sandell CG, Kizer LE, Mullins JC. Fundamental studies of direct contact latent heat energy storage. Paper presented at: Proceeding of the Annual Meeting—American Section of International Solar Energy Society; 1977; 26-30

23. Costello VA, Melsheimer SS, Edie DD. Heat transfer and calorimetric studies of a direct contact latent heat energy storage system. Presented at: the Winter Annual Meeting of the American Society of Mechanical Engineers; San Francisco; 1978; 51-60.

24. Hallet J, Keyser G. Power characteristics of a continuous crystallization latent heat recovery system. Paper presented at: International Gas Turbine Conference and Exhibit and Solar Energy Conference, the American Society of Mechanical Engineers. Paper No. 79-SOL-21, San Diego; 1979

25. Fouda AE, Despault GJG, Taylor JB, Capes CE. Solar storage systems using salt hydrate latent heat and direct contact heat exchange—I. Characteristics of pilot system operating with sodium sulphate solution. *Sol Energy*. 1980;25:437-444.

26. Lindner F, Scheunemann K. Latent heat accumulator, Patentschrift: US 4371029 A. Veröffentlichungsdatum: 1.02.1983.

27. Fouda AE, Despault GJG, Taylor JB, Capes CE. Solar storage systems using salt hydrate latent heat and direct contact heat exchange—II Characteristics of pilot system operating with sodium sulphate solution. *Solar Energy*. 1984;32:57-65.

28. Farid M, Yacoub K. Performance of direct contact latent heat storage unit. *Solar Energy*. 1989;43:237-251.

29. Inabe H, Sato K. Latent cold heat energy storage characteristics by means of direct-contact-freezing between oil droplets and cold water solution. *International Journal of Heat and Mass Transfer*. 1997;40:3189-3200.

30. Kiatsiriroata T, Tiansuwan J, Suparos T, Thalang KN. Performance analysis of a direct-contact thermal energy storage-solidification. *Renew Energy*. 2000;20:195-206.

31. Kaizawa A, Kamano H, Kawai A, et al. Thermal and flow behaviors in heat transportation container using phase change material. *Energy Convers Manag*. 2008;49:698-706.

32. Martin V, He B, Setterwall F. Direct contact PCM—water cold storage. *Appl Energy*. 2010;87:2652-2659.

33. Nogami H, Ikeuchi K, Sato K. Fundamental flow characteristics in a small columnar latent heat storage bath. *ISIJ Int*. 2010; 50:1270-1275.

34. Nomura T, Tsubota M, Oya T, Okinaka N, Akiyama T. Heat storage in direct-contact heat exchanger with phase change material. *Appl Therm Eng*. 2013;50:26-34.

35. Nomura T, Tsubota M, Sagara A, Okinaka N, Akiyama T. Performance analysis of heat storage of direct-contact heat exchanger with phase-change material. *Appl Therm Eng*. 2013; 58:108-113.

36. Nomura T, Tsubota M, Oya T, Okinaka N, Akiyama T. Heat release performance of direct-contact heat exchanger with erythritol as phase change material. *Appl Therm Eng*. 2013;61: 28-35.

37. Kunkel S, Teumer T, Dörnhofer P, et al. Determination of heat transfer coefficients in direct contact latent heat storage systems. *Appl Therm Eng*. 2018;145:71-79.

38. Lane GA. Low temperature heat storage with phase change materials. *Int J Ambient Energy*. 1980;1:155-168.

39. Galazutdinova Y, Grágeda M, Cabeza LF, Ushak S. Novel inorganic binary mixture for low-temperature heat storage applications. *Int J Energy Res*. 2017;41:2356-2364.

40. Product Information Sheet Fragoltherm Q-7, Fragol GmbH + Co. KG, Mühlheim; 2019.

41. Feldkamp L, Davis L, Kress J. Practical cone-beam algorithm. *J Opt Soc Am*. 1984;1:612-619.

42. Cabeza LF, Castell A, Barreneche C, de Gracia A, Fernández AI. Materials used as PCM in thermal energy storage in buildings: a review. *Renew Sustain Energy Rev*. 2011;15: 1675-1695.